Development of PLGA-Triiodothyronine Nanoparticles for Targeted Delivery in the Cardioprotection Against Ischemic Insult

Ozlem Ozen Karakus
Albany College of Pharmacy and Health Sciences
Noureldien H. E. Darwish
Albany College of Pharmacy and Health Sciences
Taher Salaheldin
Albany College of Pharmacy and Health Sciences
P. C. Taylor Dickinson
Albany College of Pharmacy and Health Sciences
Brian Weil
University at Buffalo Jacobs School of Medicine and Biomedical Sciences: University at Buffalo School of Medicine and Biomedical Sciences
Shaker A Mousa (shaker.mousa@acphs.edu)
Albany College of Pharmacy and Health Sciences https://orcid.org/0000-0002-9294-015X

Research

Keywords: Thyroid hormone, triiodothyronine, Nano-T3, cardiac arrest, ischemia, phosphocreatine, resuscitation.

Posted Date: August 6th, 2021

DOI: https://doi.org/10.21203/rs.3.rs-746577/v1

Abstract

Background: Ischemic heart disease is the main cause of death globally. Cardioprotection is the process whereby mechanisms that reduce myocardial damage, and activate protective factors, contribute to the preservation of the heart. Targeting these processes could be a new strategy in the treatment of post-ischemic heart failure (HF). Triiodothyronine (T3) and thyroxine (T4), which have multiple effects on the heart, prevent myocardial damage.

Results: This study describes the formulation, and characterization, of chemically modified polymeric nanoparticles incorporating T3, to target the thyroid hormone receptors. Modified T3 was conjugated to polylactide-co-glycolide (PLGA) to facilitate the active targeting of PLGA-T3. Modified T3 and PLGA-T3 was characterized with ^{1}H-NMR. Protective role of synthesized Phosphocreatine (PCr) encapsulated PLGA-T3 nanoparticles (PLGA-T3/PCr NPs) and PLGA-T3 nanoparticles (PLGA-T3 NPs) in hypoxia-mediated cardiac cell insults were investigated.

Conclusions: Data demonstrated that PLGA-T3/PCr NPs represent a potentially new therapeutic for the control of tissue damage in cardiac ischemia and resuscitation.

Introduction

Cardioprotection is a wide-ranging term that includes all mechanisms for the protection of the heart, and the multiple factors involved, such as cardiomyocytes, cytokines, cell growth, angiogenesis, and mitochondria. Many studies have shown that thyroid hormone plays an important role in cardioprotection, and its regulating mechanisms [1, 2]. The major thyroid hormone produced by the thyroid gland is L-thyroxine (T4), and when one of the iodines is removed by iodothyronine deiodinase enzymes, it forms L-triiodothyronine (T3).

T3, the most active form of thyroid hormone, is involved in cardiac protection through several mechanisms. One of these classical mechanisms is, by direct genomic signaling. When T3 binds to its nuclear receptors, by coupling to T3 response elements (TRE) in the promoter regions of target genes it regulates transcription [3]. In addition through non-genomic actions it interacts with cytoplasmic and membrane-associated, thyroid hormone receptors, namely the integrin, αvβ3, and mediates the action of thyroid hormone on the ion channels located in the cardiomyocyte membrane [4–6], to protect cells from ischemic injury [7]. By this action, T3 activates the cell surface receptor integrin αvβ3 and also leads to formation of new blood vessels (angiogenesis).

Fang et al. showed that T3 treatment improves cardioprotection against ischemia reperfusion injury in isolated rat heart cells by preserving major Ca^{2+} cycling proteins [8]. Forini et al showed that T3 treatment of isolated rat heart cells can prevent further mitochondrial disturbance and damage in ischemia [9]. They also described how T3 protects against the oxidative stress condition, by limiting p53 upregulation [10].

Thus, T3 this emerges as an attractive novel therapeutic strategy in post-ischemic heart failure (HF) [11, 12]. Although T3 appears to be a promising treatment, it has a short half-life in blood, and its genomic actions can have potentially deleterious effects. Nano-targeted delivery of T3 may prolong the circulation half-life, restrict its nuclear translocation, enhance delivery to a desired site (αvβ3), and improve its safety profile [13]. Additionally, T3 conjugated polymeric nanoparticles (NPs) allow for encapsulation of different bioactive molecules such as phosphocreatine (PCr), which is a high-energy phosphate for the myocardium, and other organs. Among polymeric NPs, polylactic acid-co-glycolic acid NPs (PLGA NPs) may play an important role in delivering hydrophobic therapeutics to the targets, such as tumor tissues. PLGAs are hydrophobic, biodegradable, FDA-approved polymers that are physically strong and highly biocompatible with free drugs, as well as other molecules such as peptides [14, 15].

A critical mechanism through which hypoxia/ischemia causes irreversible myocardial injury is by exhaustion of adenosine triphosphate (ATP). Creatine (Cr), Cyclocreatine (CCr) and their water-soluble salts Creatine-Phosphate/Phosphocreatine (CrP/PCr), and Cyclocreatine-Phosphate (CCrP) are potent bioenergetic agents that preserve high levels of ATP during ischemia. These can be encapsulated into T3 conjugated NPs. PCr is an important component in the intracellular system of energy buffering, and transfer, and provides for the high energy demands of the heart [16]. Under normal conditions, Cr is synthesized in the brain and used to form PCr through creatine kinase. PCr donates its phosphate group to adenosine diphosphate (ADP) to resynthesize adenosine triphosphate (ATP) under conditions of ATP exhaustion [17, 18]. Thus, PCr allows ATP synthesis even in the absence of oxygen and glucose [19].

Supplementation with PCr may be potentially beneficial to patients with acute and chronic myocardial ischemic injury [16, 20]. This study presents the synthesis and investigation of novel PLGA-T3 NPs, with, or without, encapsulation of PCr for potential benefits against cardiac ischemic insults.

Results

Design, Synthesis and Characterization

Thyroid hormone's effects on the cardiovascular system make it an attractive therapy for impaired hemodynamics and low levels of T3 [21]. Regulating thyroid hormone levels may be used as a therapeutic option for cardiovascular diseases. Cardioprotection by T3 may be maximized by administering PCr via T3 functionalized NPs, which could also lead to their consistent delivery. Treatment via T3 attached NPs may also change the bio-distribution, and pharmacokinetic profile, of T3 and PCr. These NPs may limit T3’s activity to the cell surface, and prolong cell membrane-mediated effects. Encapsulation of PCr by PLGA-T3 NPs may enhance the therapeutic effect of T3 by providing additional energy.

Based on the above, we designed, and synthesized, new NPs containing T3 and PCr for cardioprotection. Biocompatible, and biodegradable, copolymers of PLGA were used. The first design was to protect T3 on its amine side, and to have suitable linkers for conjugation to the PLGA polymer. Benzyl chloroformate

was used to protect the amine group because the benzyloxy carbonyl group attached nitrogen can be cleaved in hydrogen bromide/glacial acetic acid solution, without affecting the polymer PLGA chain [22]. 3-bromo propyl amine was attached to the phenolic oxygen of T3 for polymer linkage, and modified T3 was conjugated to the N-hydroxy succinimide (NHS) activated PLGA polymer (Scheme 1).

As shown in Scheme 1, the amine and carboxylic acid groups of **T3** were protected with benzyl chloroformate and methyl ester, respectively. Compounds **2** and **3** were characterized with ^{1}H-NMR and ^{13}C-NMR (**Fig. S1-4**). Compound **3** was reacted with commercially available 3-bromopropyl carbamate in the presence of potassium carbonate and ACN under reflux conditions to make compound **4** with an 87% yield. The ^{1}H-NMR spectrum of compound **4** (**Fig. S5**) exhibited three, triplet, peaks of CH_2 protons at 2.0, 3.4 and 4.0 ppm, which were assigned to the propyl group. ^{13}C-NMR spectrum is also given as a Fig.S6. Then, BOC protected propyl amine was deprotected in a 4 N HCl (in dioxane) solution, and the structure of compound **5** was confirmed with both ^{1}H and ^{13}C-NMR spectra (**Fig. S7-8**).

Compound **5** was conjugated to the PLGA polymer by its free amine group in DMSO. The resulting PLGA-T3-Cbz compound (**6**) was dialyzed using a membrane (molecular weight cutoff, 10,000 g/mol) for 2 days. The dialyzed compound (**6**) was lyophilized and dried under vacuum. The peaks of T3 aromatic protons (6.5-8 ppm), and PLGA protons in the ^{1}H-NMR spectrum, confirmed the conjugation reaction of compound **7** (**Fig. S9**). Finally, the protecting Cbz group on compound **6** was removed in HBr/CH_3COOH, and the final product PLGA-T3 (compound **7)** was dialyzed against water using a membrane (MWCO 1kDa) for 2 days.

Physicochemical Characterization of the Nanoparticles

PLGA-T3 and PLGA-T3/PCr NPs were prepared by spontaneous emulsification solvent diffusion, and modified double emulsion methods, respectively. Average particle sizes were 254 nm, 175 and 178 nm for the void, PLGA-T3 and PLGA-T3/PCr NPs respectively (**Fig S10**).

A transmission electron microscopy (TEM) image revealed the spherical morphology of the PLGA-T3/PCr NPs having an average size of 100–200 nm (Fig. 1).

Loading Percentage and Entrapment Efficiency

The PCr loading percentage of PLGA-T3/PCr NPs was determined by analyzing the amount of PCr encapsulated in the NPs, compared with the total weight of the PLGA-T3/PCr NPs. After lyophilization, 1 mg of PLGA-T3/PCr NPs powder was dispersed in 1 ml of DMSO for 10 min. Results showed that the PCr loading was 25%, while the entrapment efficiency was 93%. This reflects the success of the preparation method in preventing loss of the active drug.

Release kinetics

The release kinetics of the PCr were performed in FBS (Fetal Bovine Serum) and PBS (Phosphate Buffer Saline). A graphical representation comparing the release profiles of PLGA-T3/PCr NPs is shown in Fig. 2.

Release of the PCr was very low in PBS; at 24 h, only ~ 7% of the PCr was released. On the other hand, the maximum release in FBS was ~ 70% after 12 h.

Cardioprotective Effects of T3 and PLGA-T3/PCr NPs Under Hypoxia

Under normal conditions (normoxia) neonatal mice cardiomyocites showed contraction rates and rhythms that were similar for epinephrine, PLGA-T3 NPs and PLGA-T3 NPs/PCr (160–186 contraction/ min, regular rhythm, and multiple spots).

Under hypoxic conditions, epinephrine showed no improvement in cardiomyocyte` function (28–39 contractions/ min, irregular rhythm, and random spots). On the other hand, PLGA-T3 NPs and PLGA-T3 NPs/PCr showed significant improvement (134–145, contractions/ min, regular rhythm, and multiple spots) ($P < 0.001$ versus untreated).

Since ATP synthesis depends on the mitochondrial membrane potential, we subsequently tested to see whether PLGA-T3 NPs and PLGA-T3 NPs/PCr could protect this membrane potential. PLGA-T3 NPs and PLGA-T3 NPs/PCr significantly protected the degradation of ATP (~ 5 folds increase) ($P < 0.01$ versus T3 and T3 + PCr) (Fig. 3). Epinephrine was associated with a marked degeneration of ATP levels. These data indicate that PLGA-T3 NPs and PLGA-T3 NPs/PCr may improve glycolysis and suppress the abnormal accumulation of mitochondrial reactive oxygen species.

Similarly, under hypoxic condition**s** with PLGA-T3 NPs and PCr encapsulated PLGA-T3 NPs, troponin T levels released into the medium were decreased by 3-fold (**$P < 0.05$, and ***$P < 0.001$, respectively Fig. 4B). The results were confirmed with the confocal microscopy (Fig. 4A).

These results suggest that of PLGA-T3 NPs and PLGA-T3 NPs/PCr inhibit the damaging effect of hypoxia on cardiomyocytes.

Evaluation of free T3 and PLGA-T3 NPs-Cy7 Biodistribution in Mice.

The Cy7 signal intensity of PLGA-T3 NPs-Cy7 were detected as strong signals within 5 minutes of administration, primarily in mice brains, heart and lungs (Fig. 5).

Experimental Section

Chemicals and Analysis

4-Hydroxybenzylamine, di-*tert*-butyl di-carbonate, HCl (4 N in dioxane), N,N'-Di-Boc-1H-pyrazole-1-carboxamidine, TEA, sodium ascorbate, and copper sulfate were purchased from Sigma-Aldrich (St Louis, MO, USA). $PLGA_{5k}$-PEG_{1k}-NHS was purchased from Nano Soft Polymers (Winston-Salem, NC, USA). All

commercially available chemicals were used without further purification. Chemical structures of all synthesized compounds were confirmed with ^{1}H-NMR, ^{13}C NMR, and mass spectrometry. The NMR experiments were all performed on a Bruker Advance II 600 MHz spectrometer at the Center for Biotechnology and Interdisciplinary Studies, Rensselaer Polytechnic Institute (Troy, NY, USA). Thin layer chromatography was performed on silica gel plates with fluorescent indicators. Mass spectral analysis was performed on either an Applied Biosystems API4000 LC/MS/MS or Advion Expression CMC^{L} mass spectrometer. Analytical HPLC analyses were performed with a Waters 2695 system equipped with a Pursuit XRs C18 column (150 x 4.6 mm), with a flow rate of 1 mL/min, using a gradient of MeOH and water (0.1% TFA), and UV detection at 227 and 254 nm.

2-((benzyloxy)carbonyl)amino)-3-(4-(4-hydroxy-3-iodophenoxy)-3,5 di-iodophenyl) propanoic acid (2):

T3 (compound **1**) (1g, 1.53 mmol, 1eq) and $NaHCO_3$ (0.39 g, 4.59 mmol, 3 eq) were mixed in 20 ml THF: water (1:1) and benzyl chloroformate (0.31 g, 1.84 mmol, 1.2 eq) was added to a suspension at room temperature. After stirring for 4 h, solvents were removed under reduced pressure, and the residue was purified by column chromatography. Yield: 1.20 g, 87%.

^{1} **H-NMR (600 MHz, DMSOd6)**: 2.82 (1 H, dd, CH_2), 3.11 (1 H, dd, CH_2), 4.25 (1 H, td, CH), 5.03 (2H, s, -OCH_2), 6.60 (1H, dd, ArCH), 6.84 (1H, d, ArCH), 7.03 (1H, d, ArCH), 7.33 (3H, t, ArH-Cbz), 7.38 (2H, t, ArH-Cbz), 7.74 (1H, d, NH), 7.88 (2H, s, ArH), 10.04 (1H, s, Ar-OH). 12.89 (1H, s, COOH). ^{13}**C-NMR (150 MHz, DMSOd6)**: 35.2, 55.4, 65.9, 84.9, 92.3, 115.6, 116.5, 125.1, 127.9, 128.2, 128.8, 137.4, 139.8, 141.1, 149.5, 156.3, 173.2. **MS (ESI+)**: $C_{23}H_{18}I_3NO_6 + H^+$ Calcd, 785.83 Anal. Calcd. (%): C, 35.19; H, 2.31; N, 1.78. Found (%): C, 35.11; H, 2.22; N, 1.39.

Methyl2-(benzyloxy)carbonyl)amino)-3-(4-(4-hydroxy-3-iodophenoxy)-3,5-diiodophenyl) propanoate (3):

$SOCl_2$ (5 mL) was slowly added to a solution of compound **2** (1 g, 1.27 mmol) in MeOH (15 mL) at 0°C. The reaction mixture was refluxed at 70°C for 2 h, before cooling it to rt. MeOH was removed in vacuo and the resulting residue was poured onto ice-H_2O (25 mL), and extracted with DCM (2 x 10 mL). The combined organic extracts were washed with 10% $NaHCO_3$ (2 x 10 mL), and brine, and dried (Na_2SO_4), and concentrated to provide the product as a white solid. Yield: 1.02 g, 85%.

^{1} **H-NMR (600 MHz, DMFd6)**: 3.03 (1 H, dd, CH_2), 3.24 (1 H, dd, CH_2), 3.52 (3H, s, -OCH_3), 4.53 (1 H, td, CH), 5.09 (2H, s, -OCH_2), 6.69 (1H, dd, ArCH), 6.99 (1H, d, ArCH), 7.15 (1H, d, ArCH), 7.36 (3H, t, ArH-Cbz), 7.41 (2H, t, ArH-Cbz), 7.82 (1H, d, NH), 8.01 (2H, s, ArH), 10.39 (1H, s, Ar-OH). ^{13}**C-NMR (150 MHz, DMFd6)**: 35.3, 51.8, 55.5, 65.9, 83.9, 91.2, 115.2, 116.4, 125.2, 127.6, 127.8, 128.5, 137.3, 139.3, 141.3, 149.6, 152.7, 156.4, 172.0 **MS (ESI+)**: $C_{24}H_{20}I_3NO_6 + H^+$ Calcd, 799.84 Anal. Calcd. (%): C, 36.07; H, 2.52; N, 1.75. Found (%): C, 36.23; H, 2.39; N, 1.66.

Methyl2-(benzyloxy)carbonyl)amino)-3-(4-(4-(3-(tert-butoxycarbonyl)amino) propoxy)-3-iodophenoxy)-3,5-diiodophenyl)propanoate (4):

K_2CO_3 (275 mg, 1.99 mmol, 3 eq) was added with stirring to a solution of compound **3** (530 mg, 0.66 mmol, 1 eq) in ACN (25 mL) at rt. After the reaction mixture was stirred for 30 min, tert-butyl (3-bromopropyl) carbamate (0.19 g, 0.79 mmol, 1.2 eq) was added to the mixture and the temperature was increased to 80ºC, and refluxed for 24 h. The solution was filtered to remove excess K_2CO_3. Solvents were removed under reduced pressure, and the oily residue was purified by column chromatography. Yield: 536 mg, 85%.

^{1} **H-NMR (600 MHz, $CDCl_3$)**: 1.46 (9H, s, $-CH_3$), 2.05 (2H, m, $-CH_2-$), 3.01 (1 H, dd, $-CH_2$), 3.11 (1 H, dd, $-CH_2$), 3.42 (2H, t, $-CH_2-$), 3.79 (3H, s, $-OCH_3$), 4.03 (2H, t, $-CH_2-$), 4.66 (1 H, td, -CH), 5.15 (2H, s, $-OCH_2$), 5.42 (1H, s, NH), 6.68 (1H, dd, ArCH), 6.73 (1H, d, ArCH), 7.28 (1H, d, ArH), 7.35 (1H, d, ArH-Cbz), 7.38 (2H, d, ArH-Cbz), 7.39 (2H, d, ArH-Cbz), 7.66 (2H, s, ArH). ^{13}**C-NMR (150 MHz, $CDCl_3$)**: 28.4, 29.2, 36.9, 38.5, 52.6, 54.7, 67.2, 68.2, 79.0, 86.7, 90.9, 112.0, 115.7, 126.5, 128.1, 128.3, 128.6, 136.0, 137.1, 141.0, 150.5, 152.9, 155.5, 156.0, 171.3 **MS (ESI+)**: $C_{32}H_{35}I_3N_2O_8 + H^+$ Calcd, 956.95 Anal. Calcd. (%): C, 40.19; H, 3.69; N, 2.93. Found (%): C, 40.25; H, 3.54; N, 2.79.

3-(4-(4-(3-aminopropoxy)-3-iodophenoxy)-3,5-diiodophenyl)-2 ((benzyloxy)carbonyl)amino) propanoic acid (5):

LiOH (173 mg, 7.2 mmol) was added to a mixture of compound **4** (400 mg, 0.42 mmol) in 20 ml THF: water (1:1) and stirred 2h at room temperature. The mixture was acidified to pH = 5 with HCl (1 M), extracted with DCM (2x100 mL), and washed with water (100 mL) and then brine. The solution was dried over magnesium sulfate, filtered, and concentrated to give a white solid. Yield: 468 mg, 85%. Crude product (325 mg, 0.57 mmol) was dissolved in 3 mL anhydrous 1,4-dioxane and 3 mL HCl (4 N in dioxane) and stirred at room temperature. After 24 h, the solvent was removed under reduced pressure, and the oily residue was precipitated by stirring in diethyl ether to afford compound **5** as a yellowish solid. Yield 240 mg, 90%.

^{1} **H-NMR (600 MHz, DMSOd6)**: 2.10 (2H, m, $-CH_2-$), 2.81 (1 H, dd, $-CH_2-$), 2.88 (1 H, m, $-CH_2$), 3.00 (2H, t, $-CH_2-$), 4.09 (2H, t, $-CH_2-$), 4.25 (1 H, td, -CH), 5.01 (2H, s, $-OCH_2$), 6.68 (1H, dd, ArCH), 6.98 (1H, d, ArCH), 7.14 (1H, d, ArH), 7.31 (3H, m, ArH-Cbz), 7.37 (2H, m, ArH-Cbz), 7.70 (1H, s, NH), 7.89 (2H, s, ArH). ^{13}**C-NMR (150 MHz, DMSOd6)**: 27.2, 30.3, 35.2, 36.5, 42.8, 55.6, 65.8, 66.6, 87.6, 92.5, 113.6, 116.1, 125.5, 127.8, 128.2, 128.8, 137.4, 140.1, 141.0, 150.8, 152.0, 152.7, 156.4, 173.1 **MS (ESI+)**: $C_{26}H_{25}I_3N_2O_8 + H^+$ Calcd, 841.88 Anal. Calcd. (%): C, 37.08; H, 2.99; N, 3.33. Found (%): C, 37.15; H, 2.54; N, 3.48.

Compound 6 and 7

Compound **5** (100 mg, 1 eq) and 1 eq of PLGA5k-NHS were dissolved in 5 mL DMSO (4:1) and stirred for 24 h at rt. to form Compound **6**. Compound **6** was then dialyzed against water using a membrane (MWCO 1kDa) for 2 days, Yield: 523 mg, 60%.

2ml HBr (in 33% AcOH) was added to compound **6** (100 mg, 1 eq) in 5 mL DCM and stirred at rt for 1 h. After removing the solvent, crude compound **7** was dialyzed against water using a membrane (MWCO 1kDa) for 2 days. Yield: 600 mg, 60%.

^{1} **H-NMR (600 MHz, DMSOd6)**: 2.10 (2H, m, -CH_2-), 2.81 (1 H, dd, -CH_2-), 2.88 (1 H, m, -CH_2), 3.00 (2H, t, -CH_2-), 4.09 (2H, t, -CH_2-), 4.25 (1 H, td, -CH), 5.01 (2H, s, -OCH_2), 6.68 (1H, dd, ArCH), 6.98 (1H, d, ArCH), 7.14 (1H, d, ArH), 7.31 (3H, m, ArH-Cbz), 7.37 (2H, m, ArH-Cbz), 7.70 (1H, s, NH), 7.89 (2H, s, ArH).

Synthesis and Characterization of PLGA-T3 NPs

PLGA-T3 NPs were synthesized by a modified spontaneous emulsification solvent diffusion method (SESD) in which they were effectively obtained by forming a nanoscale shell made from nontoxic polyvinyl alcohol (PVA) around PLGA-T3 under mechanical stirring [23, 24].

The typical operating procedure was as follows; 1. 200 mg of PLGA-T3 was dissolved in 1 ml DMSO. The obtained polymer solution was then added (20 ul / min) into 40 ml of aqueous 1% PVA solution in a 100-ml glass flask while continuously stirring at 600 rpm for 2 hrs. The prepared nanoparticles were then harvested, and washed, three times by centrifugation at 8000 rpm and re-dispersed in 5 ml purified water for further characterization. The aqueous dispersed PLGA-T3 NPs were then freeze-dried in a vacuum to obtain powdered NPs.

Synthesis of PLGA-T3/ PCr NPs

PCr encapsulated PLGA-T_3 nanoparticles were synthesized by a modified combined double emulsion method in which PLGA-T3 NPs/PCr were effectively obtained by forming nanoscale shells made from PVA around PLGA-T3 NPs/PCr under mechanical stirring [23, 24]. The typical operating procedure was as follows; 200 mg of PLGA-T3 and 45 mg PCr were dissolved in 1 ml DMSO. The obtained polymer solution was then added (20 ul / min) into 20 ml of aqueous 1% PVA solution under continuous stirring, at 600 rpm, for 2 hrs. This solution then was added to 50 ml 0.5 % PVA under stirring for 24 h. PLGA-T3 NPs/PCr were harvested, and washed, three times, by centrifugation at 8000 rpm, and re-dispersed in 5 ml purified water for further characterization. The aqueous dispersed PLGA-T3/PCr NPs were then freeze-dried in a vacuum to obtain the powdered NPs.

Characterization of the Prepared PLGA-T3/PCr NPs

Zeta sizer (Malvern Instrumentation Co, Westborough, MA, USA) was used to determine the size distribution and zeta potential of the nano capsules in the aqueous dispersion. High Resolution Transmission Electron Microscope (HRTEM) was used for topographic imaging. 20 µl of a diluted NP dispersion was placed on 300 mesh carbon coated grid, left to dry for 15 mins, then fixed on the platinum sample holder for TEM imaging under 200 KV. The T3 concentration was measured by HPLC.

Encapsulation Efficiency (EE) and Loading Ratio (LR)

The encapsulation efficiency was calculated by analyzing the T3 loading in the NPs. After lyophilization, the weighed NP powder was dispersed in 3 mL of DMSO for 10 minutes. The amount of T3 in the DMSO was determined by using HPLC.

$$\text{Encapsulation Efficiency (EE)} = \frac{\text{T3 concentration in NP}}{\text{Initial T3 concentration}} \times 100$$

The loading ratio of the PLGA-T3 NPs was determined by measuring the amount of T3 in the nanoparticles, and the weight of the whole nanoparticle [25].

$$\text{Loading efficiency} = \frac{\text{T3 concentration in NP}}{\text{Total weight of NP}} \times 100$$

In Vitro Release Study

The release kinetics studies were performed in FBS and PBS. A known amount of the PLGA-T3/Pcr NPs was suspended in 15 ml of PBS/FBS. The solutions were incubated at 37 ℃. At pre-determined time intervals over a week. 500 µl of the solution was filtered through Millipore tubes containing a 30 kD membrane to separate the released PCr from the NPs and was analyzed by HPLC.

Evaluation of the Cardioprotective Effect of T3 and PLGA-T3/PCr NPs Under Hypoxia

The cardioprotective effect of T3 and PLGA-T3/PCr NPs under hypoxia were studied using isolated neonatal mice cardiomyocytes using a Pierce™ Primary Cardiomyocyte Isolation Kit (ThermoFisher, Waltham, MA, USA). Isolation of neonatal mice cardiomyocytes were performed as previously described [26], and all methods described in this protocol have been approved by the Animal Care and Use Committee (IACUC), and adhere to federal, and state, regulations.

All steps were performed in a sterile laminar flow cell culture hood. This protocol is intended for the isolation of neonatal mouse hearts from approximately 8–10 pups. Briefly, freshly dissected neonatal hearts were immediately placed into separate 1.5 mL sterile microcentrifuge tubes with 500 µL ice cold Hanks' Balanced Salt solution (HBSS). Each heart was minced into 1-3mm^3 pieces, and washed twice with ice cold HBSS to remove blood from the tissue. The cardiomyocytes were incubated with a Cardiomyocyte Isolation Enzymes in a 37°C incubator for 30 minutes.

After washing, complete Dulbecco's Modified Eagle Medium (DMEM) for Primary Cell Isolation was added to each tube and the solutions were pipetted up and down using a sterile 1.0 mL pipette tip. After the tissue was primarily a single-cell suspension, an additional 1.0 mL of complete DMEM was added for

Primary Cell Isolation to each tube to bring the total volume to 1.5 mL. After evaluation of the cell concentration and viability, the cells were allowed to grow in 35 mm sterile culture dishes.

After 2 days, the cardiomyocytes were treated with PBS (control), T3 (1–3 μM), T3 + PCr (5 μM), PLGA-T3 NPs (1–3 μM), PLGA-T3/PCr NPs (5 μM), and Epinephrine (0.5 μM). The cells were cultured in a hypoxia incubator with 4% oxygen, 5% CO_2 at 37°C for 24 h and compared with normoxia conditions.

Mitochondrial function, and sarcomere integrity, were studied using an ATP– bioluminescence assay (ATP Bioluminescence assay kit HS II, Roche Life Science, Indianapolis, IN, USA) following the manufacturer's instructions. Mice neonatal cardiomyocytes were incubated with a cell lysis reagent (Sigma, Fremont, CA, USA), and protease inhibitor cocktail (Sigma), for 5 min at rt, in darkness. Luciferase reagent was added to the samples, and the luminescence of the live cells was measured by the GloMax Luminometer (Promega Corporation, WI, USA). After adding troponin T antibody conjugated with Fluorescein isothiocyanate (FITC) (BD bioscience, San Jose, CA, USA), cardiac troponin T levels were measured using flow cytometry. Confirmation was done by Immunostaining with anti-Troponin T-PE (BD bioscience, USA), using confocal microscopy (LeicaTCS SP5, Wetzlar, Germany). Photographic and fluorescent images were taken at constant exposure time for evaluation of cardiac troponin T levels. Cells were imaged at an excitation wavelength of 488 nm; emission was detected between 505 nm and 560 nm.

Biodistribution of T3 and PLGA-T3 NPs-Cy7

Animal studies were conducted at the animal facility of the Veterans Affairs Medical Center, Albany, NY, USA, and approved by the IACUC committee of the Veterans Affairs Medical Center. Female Balb C mice aged 5–6 weeks and weighing 18–20 g, were purchased from Taconic Biosciences Inc. (Hudson, NY, USA). Mice were maintained under specific pathogen-free conditions, and housed under controlled temperature (20–24°C), humidity (60–70%), and 12 h light/dark cycle with access to water and food ad libitum. Mice were allowed to acclimatize for 5 days before the study.

Mice were injected (300 μL/mouse) with PLGA-T3/PCr NPs and free T3 labeled with Cy7 into the tail vein. Biodistribution of T3 was evaluated immediately at (0), 1, 2, 4 and 24 h using an *in vivo* imaging system (IVIS®, Perkin Elmer, Boston, MA, USA). PBS was injected as the control, and all mice were imaged before injection, to assess the background signals.

Statistical Analysis

An overall comparison of the means for all groups was done using a one-way ANOVA. Tukey confidence intervals were used to test for differences in means for each experimental group versus the control group. Results are presented as means ± S.D. A value of $P < 0.05$ indicated a statistically significant difference.

Discussion

Several studies have shown that thyroid hormones play a crucial role in cardioprotection after HF, because of their effects on molecular pathways and cardiac function and structure. PLGA-T3, a nanoparticle which incorporates T3, may be the first of a new class of therapeutic agents. It utilizes the biological properties inherent in the relationship between T3 and its αvβ3 membrane receptor [27, 28], and preferentially attaches to the receptor in hypoxic cells. The hypoxic and acidic medium of the ischemic heart may be a reason for the enhanced NP degradation, and drug release [29, 30].

The major activity of PLGA-T3/PCr NPs appears to be the delivery of energy to an energy depleted cell. In cardiac arrest (CA) oxidative phosphorylation stops and, as a result, both ATP and PCr, critical contributors to cellular energy utilization, are depleted within a few minutes [31–33]. PLGA-T3/PCr NPs may provide energy to the cell, until normal oxidative phosphorylation can be restored.

PLGA-T3/PCr NPs can improve the energy status in two ways. The first is initiated by PLGA-T3/PCr NP itself. It is configured to present T3 to the membrane receptor αvβ3 in such a manner that only the T3's non-genomic properties are activated [34, 35]. This activation provides the energy to activate a series of plasma membrane ion pumps. T3 is an important regulator of several cell surface ion pumps crucial to cardiac resuscitation. These include Na/K-ATPase, the Na+/H + antiporter and Ca + 2-ATPase. Activation of these pumps restores cell membrane electrical potentials, thus initiating cell contraction [36]. This action also introduces energy into the cytoplasm to help restore mitochondrial activity [37]. The second is the incorporation of PCr within the architecture of PLGA-T3/PCr NP. When the PCr released upon contact with the αvβ3 receptor [38, 39], it is immediately carried into the cell cytoplasm where creatine kinase, located mainly in the cristae of the plasma membrane of the mitochondria [40], play an important role in the regulation of the cellular energy homeostasis. The phosphate delivers energy to the cell by phosphorylation of ADP to make ATP, as well as other phosphate dependent reactions involved in the delivery of energy within the cell [41]. Delivering PCr to the cell fulfills many of its acute energy needs, thereby facilitating the cell's survival.

Forini, et al., considered the cardio protective effects of T3 in ischemic condition. They showed that T3 treatment can prevent further mitochondrial disturbances and damage, in ischemic cases, and thoroughly described the T3 cardio protective effects, particularly on **oxidative stress** conditions [9, 10]. Similarly, Lin et al., demonstrated that T3, but not T4, increase Src/PI3K phosphorylation through integrin αvβ3 in human glioma cells [42]. PLGA-T3/PCr NPs may elicit their actions by a non-classical mechanism, without direct gene transcription regulation by nuclear TRs (spell out). These non-genomic actions of PLGA-T3/PCr NPs may be mediated indirectly by modulating gene function.

Furthermore, in consistent with our results, regarding the rapid distribution of PLGA-T3-Cy into brain, and heart/lung tissue, Davis et al., discussed the neuroprotective effects of thyroid hormone including the upregulation of the seladin-1 gene, which is associated with anti- apoptotic activity. In addition, the T4 serum transport protein, Transthyretin, has been found to be neuroprotective in the setting of brain ischemia indicating that it rapidly penetrates the blood brain barrier. TTR (Transthyretin) gene expression has also been reported to be upregulated in ischemic brain tissue, in TTR null mice [43].

Finally, PLGA-T3 NPs may have advantages over the conventional (e.g., epinephrine) for ischemic heart disease, not only by its cardioprotective effects, but also by its neuroprotective effects.

Declarations

Ethics approval and consent to participate: N/A

Consent for publication: All authors approved the submission

Availability of data and materials: Data are provided in the manuscript and its supplement. Additional figures showing ^{1}H-NMR and ^{13}C-NMR spectra of the synthesized compounds.

Raw data are available on file at the Pharmaceutical Research Institute at ACPHS.

Competing interests: No competing interest to be declared

Funding: Partial funding provided by Pro-Al Medico Technologies Inc and the Pharmaceutical Research Institute at ACPHS.

Authors' contributions: Ozlem Ozen Karakus contributed to the conjugation chemistry of T3 to PLGA, data analysis, and writing manuscript draft; Noureldien H. E. Darwish contributed to the cardioprotective and neuroprotective biological evaluations as well as T3 NP biodistribution; Taher Salaheldin contributed to the Nano assembly of T3NP, characterization and release kinetics ; P. C. Taylor Dickinson contributed to the discussions of the data; Brian Weil contributed to data review and in depth data discussions; and Shaker A Mousa contributed to the overall design, supervision, data interpretation, analysis, writing the final integrated manuscript.

Acknowledgements: Funding was received from both Pro-Al Medico Technologies Inc., Suffern, NY and from the Pharmaceutical Research Institute (PRI) at Albany College of Pharmacy and Health Sciences. Special thanks to Dr. Mehdi Rajabi for his initial help on the synthesis of the compounds.

References

1. Pantos, C.; Mourouzis, I.; Markakis, K.; Dimopoulos, A.; Xinaris, C.; Kokkinos, A.D.; Panagiotou, M.; Cokkinos, D.V. Thyroid hormone attenuates cardiac remodeling and improves hemodynamics early after acute myocardial infarction in rats. *Eur J Cardiothorac Surg* **2007**, *32*, 333-339, doi:10.1016/j.ejcts.2007.05.004.
2. Zhang, Y.; Dedkov, E.I.; Lee, B., 3rd; Li, Y.; Pun, K.; Gerdes, A.M. Thyroid hormone replacement therapy attenuates atrial remodeling and reduces atrial fibrillation inducibility in a rat myocardial infarction-heart failure model. *J Card Fail* **2014**, *20*, 1012-1019, doi:10.1016/j.cardfail.2014.10.003.
3. Zoeller, R.T. Neuroendocrine Regulation of Development, Growth and Metabolism–Thyroid. In *Handbook of neuroendocrinology*; Elsevier: 2012; pp. 259-270.

4. Razvi, S. Novel uses of thyroid hormones in cardiovascular conditions. *Endocrine* **2019**, *66*, 115-123, doi:10.1007/s12020-019-02050-4.
5. Davis, P.J.; Lin, H.Y.; Hercbergs, A.A.; Keating, K.A.; Mousa, S.A. How thyroid hormone works depends upon cell type, receptor type, and hormone analogue: implications in cancer growth. *Discov Med* **2019**, *27*, 111-117.
6. Jabbar, A.; Pingitore, A.; Pearce, S.H.; Zaman, A.; Iervasi, G.; Razvi, S. Thyroid hormones and cardiovascular disease. *Nat Rev Cardiol* **2017**, *14*, 39-55, doi:10.1038/nrcardio.2016.174.
7. Davis, P.J.; Leonard, J.L.; Lin, H.Y.; Leinung, M.; Mousa, S.A. Molecular Basis of Nongenomic Actions of Thyroid Hormone. *Vitam Horm* **2018**, *106*, 67-96, doi:10.1016/bs.vh.2017.06.001.
8. Fang, L.; Xu, Z.; Lu, J.; Hong, L.; Qiao, S.; Liu, L.; An, J. Cardioprotective effects of triiodothyronine supplementation against ischemia reperfusion injury by preserving calcium cycling proteins in isolated rat hearts. *Exp Ther Med* **2019**, *18*, 4935-4941, doi:10.3892/etm.2019.8114.
9. Forini, F.; Kusmic, C.; Nicolini, G.; Mariani, L.; Zucchi, R.; Matteucci, M.; Iervasi, G.; Pitto, L. Triiodothyronine prevents cardiac ischemia/reperfusion mitochondrial impairment and cell loss by regulating miR30a/p53 axis. *Endocrinology* **2014**, *155*, 4581-4590, doi:10.1210/en.2014-1106.
10. Forini, F.; Nicolini, G.; Iervasi, G. Mitochondria as key targets of cardioprotection in cardiac ischemic disease: role of thyroid hormone triiodothyronine. *Int J Mol Sci* **2015**, *16*, 6312-6336, doi:10.3390/ijms16036312.
11. Heusch, G. Molecular basis of cardioprotection: signal transduction in ischemic pre-, post-, and remote conditioning. *Circ Res* **2015**, *116*, 674-699, doi:10.1161/CIRCRESAHA.116.305348.
12. Pingitore, A.; Iervasi, G.; Forini, F. Role of the Thyroid System in the Dynamic Complex Network of Cardioprotection. *Eur Cardiol* **2016**, *11*, 36-42, doi:10.15420/ecr.2016:9:2.
13. Sudha, T.; Bharali, D.J.; Yalcin, M.; Darwish, N.H.; Coskun, M.D.; Keating, K.A.; Lin, H.Y.; Davis, P.J.; Mousa, S.A. Targeted delivery of cisplatin to tumor xenografts via the nanoparticle component of nano-diamino-tetrac. *Nanomedicine (Lond)* **2017**, *12*, 195-205, doi:10.2217/nnm-2016-0315.
14. Rezvantalab, S.; Drude, N.I.; Moraveji, M.K.; Guvener, N.; Koons, E.K.; Shi, Y.; Lammers, T.; Kiessling, F. PLGA-Based Nanoparticles in Cancer Treatment. *Front Pharmacol* **2018**, *9*, 1260, doi:10.3389/fphar.2018.01260.
15. Makadia, H.K.; Siegel, S.J. Poly Lactic-co-Glycolic Acid (PLGA) as Biodegradable Controlled Drug Delivery Carrier. *Polymers (Basel)* **2011**, *3*, 1377-1397, doi:10.3390/polym3031377.
16. Landoni, G.; Zangrillo, A.; Lomivorotov, V.V.; Likhvantsev, V.; Ma, J.; De Simone, F.; Fominskiy, E. Cardiac protection with phosphocreatine: a meta-analysis. *Interact Cardiovasc Thorac Surg* **2016**, *23*, 637-646, doi:10.1093/icvts/ivw171.
17. Wyss, M.; Kaddurah-Daouk, R. Creatine and creatinine metabolism. *Physiol Rev* **2000**, *80*, 1107-1213, doi:10.1152/physrev.2000.80.3.1107.
18. Rawson, E.S.; Venezia, A.C. Use of creatine in the elderly and evidence for effects on cognitive function in young and old. *Amino Acids* **2011**, *40*, 1349-1362, doi:10.1007/s00726-011-0855-9.

19. Li, T.; Wang, N.; Zhao, M. Neuroprotective effect of phosphocreatine on focal cerebral ischemia-reperfusion injury. *J Biomed Biotechnol* **2012**, *2012*, 168756, doi:10.1155/2012/168756.
20. Strumia, E.; Pelliccia, F.; D'Ambrosio, G. Creatine phosphate: pharmacological and clinical perspectives. *Adv Ther* **2012**, *29*, 99-123, doi:10.1007/s12325-011-0091-4.
21. Gomberg-Maitland, M.; Frishman, W.H. Thyroid hormone and cardiovascular disease. *Am Heart J* **1998**, *135*, 187-196, doi:10.1016/s0002-8703(98)70081-x.
22. He, Z.; Sun, Y.; Cao, J.; Duan, Y. Degradation behavior and biosafety studies of the mPEG-PLGA-PLL copolymer. *Phys Chem Chem Phys* **2016**, *18*, 11986-11999, doi:10.1039/c6cp00767h.
23. Murakami, H.; Kobayashi, M.; Takeuchi, H.; Kawashima, Y. Preparation of poly(DL-lactide-co-glycolide) nanoparticles by modified spontaneous emulsification solvent diffusion method. *Int J Pharm* **1999**, *187*, 143-152, doi:10.1016/s0378-5173(99)00187-8.
24. Sudha, T.; Bharali, D.J.; Yalcin, M.; Darwish, N.H.; Debreli Coskun, M.; Keating, K.A.; Lin, H.Y.; Davis, P.J.; Mousa, S.A. Targeted delivery of paclitaxel and doxorubicin to cancer xenografts via the nanoparticle of nano-diamino-tetrac. *Int J Nanomedicine* **2017**, *12*, 1305-1315, doi:10.2147/IJN.S123742.
25. Sudha, T.; Bharali, D.J.; Yalcin, M.; Darwish, N.H.; Coskun, M.D.; Keating, K.A.; Lin, H.-Y.; Davis, P.J.; Mousa, S.A. Targeted delivery of paclitaxel and doxorubicin to cancer xenografts via the nanoparticle of nano-diamino-tetrac. *International journal of nanomedicine* **2017**, *12*, 1305.
26. Ehler, E.; Moore-Morris, T.; Lange, S. Isolation and culture of neonatal mouse cardiomyocytes. *J Vis Exp* **2013**, doi:10.3791/50154.
27. Cody, V.; Davis, P.J.; Davis, F.B. Molecular modeling of the thyroid hormone interactions with αvβ3 integrin. *Steroids* **2007**, *72*, 165-170.
28. Debreli Coskun, M.; Sudha, T.; Bharali, D.J.; Celikler, S.; Davis, P.J.; Mousa, S.A. αvβ3 Integrin Antagonists Enhance Chemotherapy Response in an Orthotopic Pancreatic Cancer Model. *Frontiers in pharmacology* **2020**, *11*, 95, doi:10.3389/fphar.2020.00095.
29. Mousa, S.A.; Sallam, A.; Darwish, N. Cardiovascular Protective Effect of Thyroxine and Nano-Thyroxine Against Ischemic Insults. *Circulation* **2019**, *140*, A133-A133.
30. Mitchell, M.J.; Billingsley, M.M.; Haley, R.M.; Wechsler, M.E.; Peppas, N.A.; Langer, R. Engineering precision nanoparticles for drug delivery. *Nature Reviews Drug Discovery* **2020**, 1-24.
31. Morton, A.R. Chapter 8 - Exercise Physiology. In *Pediatric Respiratory Medicine (Second Edition)*, Taussig, L.M., Landau, L.I., Eds.; Mosby: Philadelphia, 2008; pp. 89-99.
32. Jafri, M.S.; Dudycha, S.J.; O'Rourke, B. Cardiac energy metabolism: models of cellular respiration. *Annual review of biomedical engineering* **2001**, *3*, 57-81, doi:10.1146/annurev.bioeng.3.1.57.
33. Abd-Elfattah, A.S.; Tuchy, G.E.; Jessen, M.E.; Salter, D.R.; Goldstein, J.P.; Brunsting III, L.A.; Wechsler, A.S. Hot shot induction and reperfusion with a specific blocker of the es-ENT1 nucleoside transporter before and after hypothermic cardioplegia abolishes myocardial stunning in acutely ischemic hearts despite metabolic derangement: Hot shot drug delivery before hypothermic cardioplegia. *The Journal of thoracic and cardiovascular surgery* **2013**, *146*, 961-970. e963.

34. Davis, P.J.; Lin, H.-Y.; Hercbergs, A.A.; Keating, K.A.; Mousa, S.A. How Thyroid Hormone Works Depends on Cell Type, Receptor Type, and Hormone Analogue: Implications in Cancer Growth. *Discovery medicine* **2019**, *27*, 111-117.
35. Davis, P.J.; Ashur-Fabian, O.; Incerpi, S.; Mousa, S.A. Non Genomic Actions of Thyroid Hormones in Cancer. *Frontiers in Endocrinology* **2019**, *10*.
36. Lei, J.; Nowbar, S.; Mariash, C.N.; Ingbar, D.H. Thyroid hormone stimulates Na-K-ATPase activity and its plasma membrane insertion in rat alveolar epithelial cells. *American journal of physiology. Lung cellular and molecular physiology* **2003**, *285*, L762-772, doi:10.1152/ajplung.00376.2002.
37. Davis, P.J.; Davis, F.B.; Cody, V. Membrane receptors mediating thyroid hormone action. *Trends in Endocrinology & Metabolism* **2005**, *16*, 429-435.
38. van der Meel, R.; Vehmeijer, L.J.; Kok, R.J.; Storm, G.; van Gaal, E.V. Ligand-targeted particulate nanomedicines undergoing clinical evaluation: current status. *Advanced drug delivery reviews* **2013**, *65*, 1284-1298.
39. Iyer, A.K.; Singh, A.; Ganta, S.; Amiji, M.M. Role of integrated cancer nanomedicine in overcoming drug resistance. *Advanced drug delivery reviews* **2013**, *65*, 1784-1802.
40. Kottke, M.; Wallimann, T.; Brdiczka, D. Dual electron microscopic localization of mitochondrial creatine kinase in brain mitochondria. *Biochemical medicine and metabolic biology* **1994**, *51*, 105-117.
41. Gaddi, A.; Galuppo, P.; Yang, J. Creatine phosphate administration in cell energy impairment conditions: a summary of past and present research. *Heart, Lung and Circulation* **2017**, *26*, 1026-1035.
42. Lin, H.-Y.; Sun, M.; Tang, H.-Y.; Lin, C.; Luidens, M.K.; Mousa, S.A.; Incerpi, S.; Drusano, G.L.; Davis, F.B.; Davis, P.J. L-Thyroxine vs. 3, 5, 3'-triiodo-L-thyronine and cell proliferation: activation of mitogen-activated protein kinase and phosphatidylinositol 3-kinase. *American Journal of Physiology-Cell Physiology* **2009**, *296*, C980-C991.
43. Davis, P.; Lin, H.-Y.; Davis, F.; Luidens, M.; Mousa, S.; Cao, J.; Zhou, M. Molecular Basis for Certain Neuroprotective Effects of Thyroid Hormone. *Frontiers in Molecular Neuroscience* **2011**, *4*, doi:10.3389/fnmol.2011.00029.

Figures

Figure 1

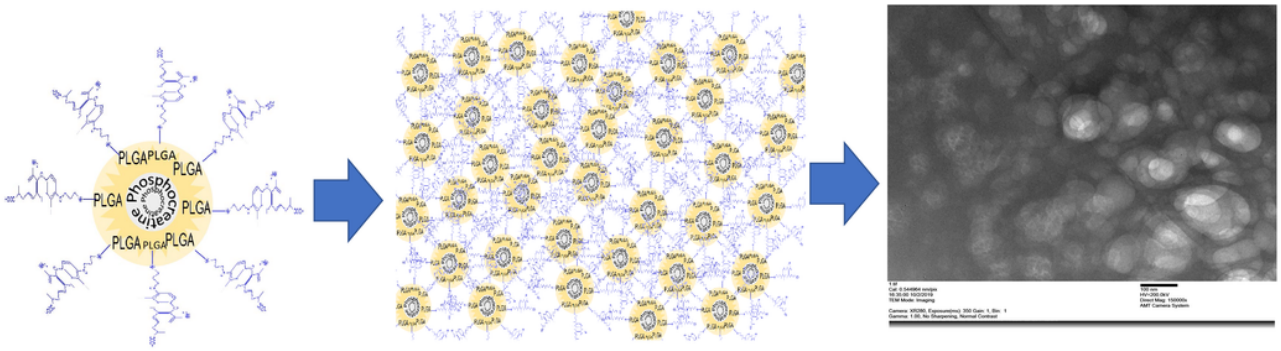

Figure 1

Schematic draw and TEM image of PLGA-T3/PCr NPs.

Figure 2

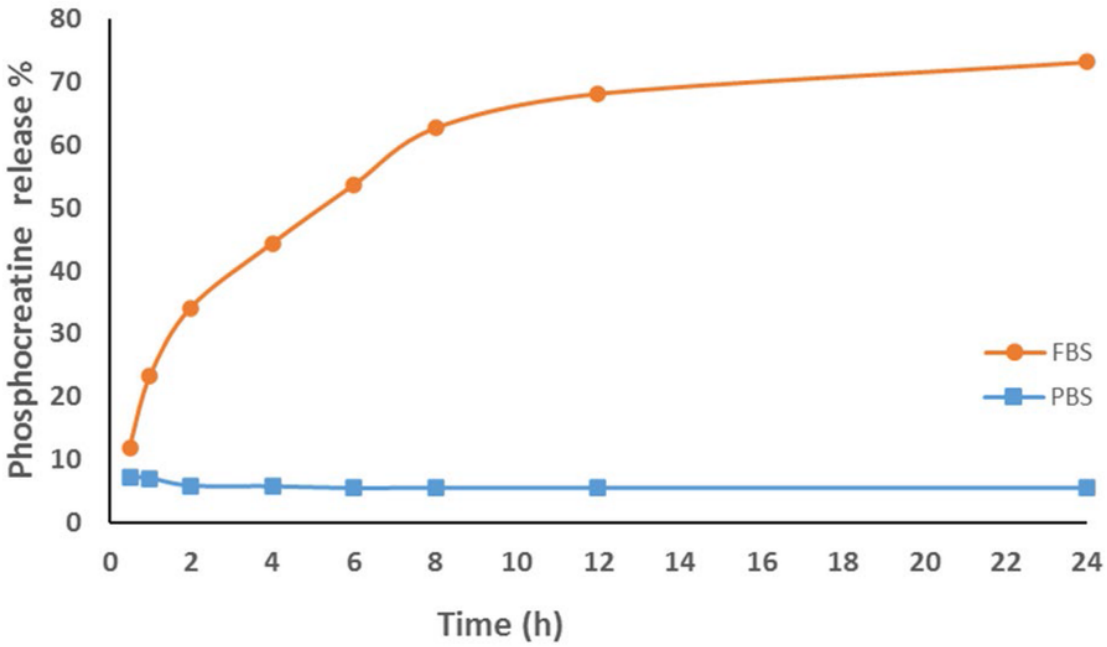

Figure 2

In vitro release kinetics of PCr from PLGA-T3 NPs/PCr in FBS and PBS using HPLC.

Figure 3

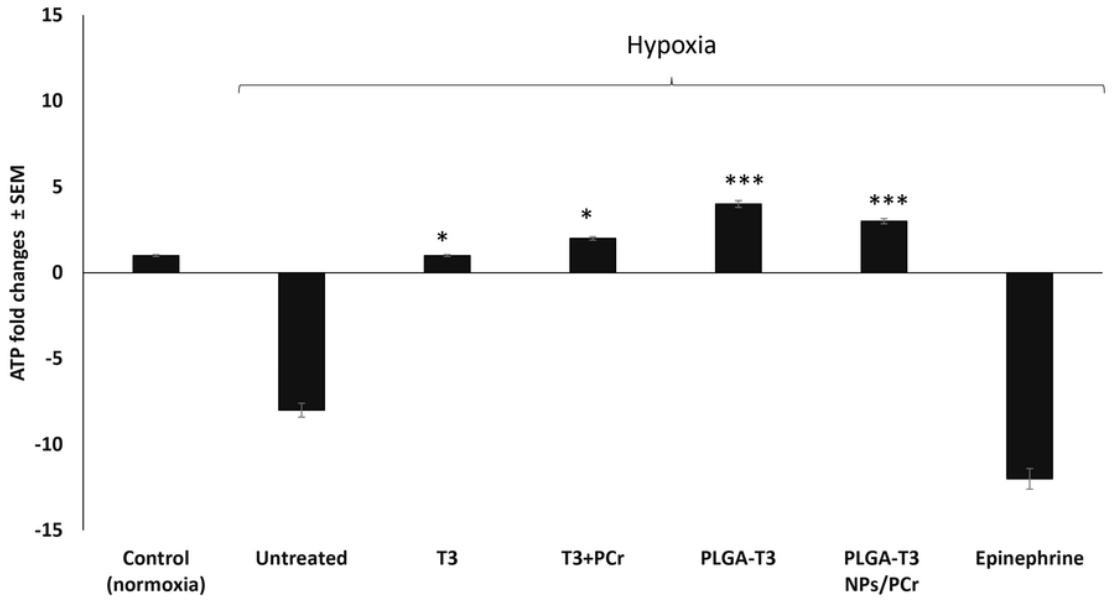

Figure 3

Cardioprotective effect of T3, PLGA-T3 NPs with or without PCr in normoxia vs hypoxic conditions. ATP levels in neonatal cardiomyocytes (bioluminescence assay), *P<0.01 versus hypoxia.

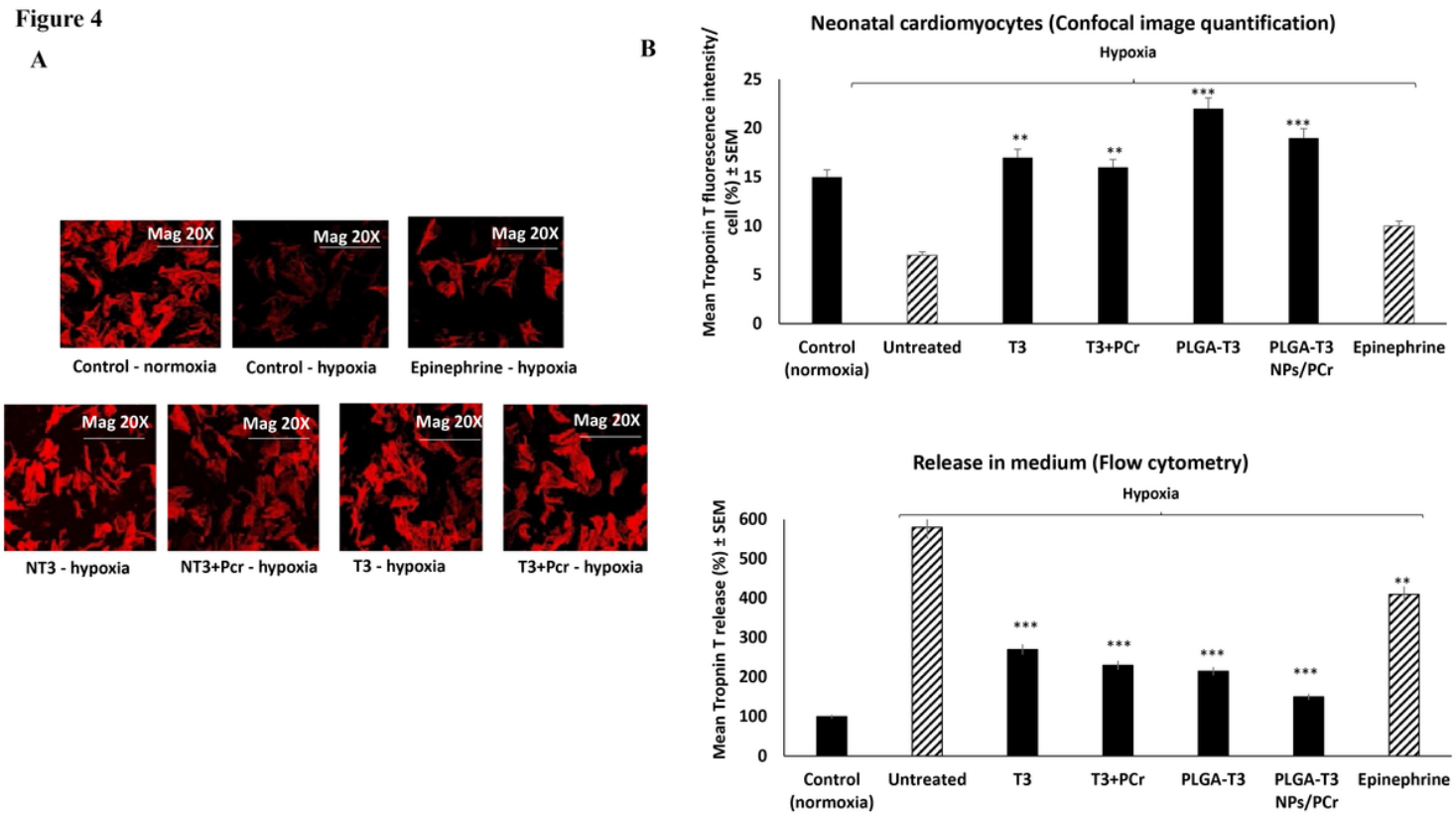

Figure 4

Expression of Troponin T in neonatal cardiomyocytes under hypoxic condition. A) Immunostaining by anti-Troponin T-PE (confocal microscopy). B) Quantitation of troponin T in neonatal cardiomyocyte and in medium. **P<0.05, ***P<0.001 versus hypoxia.

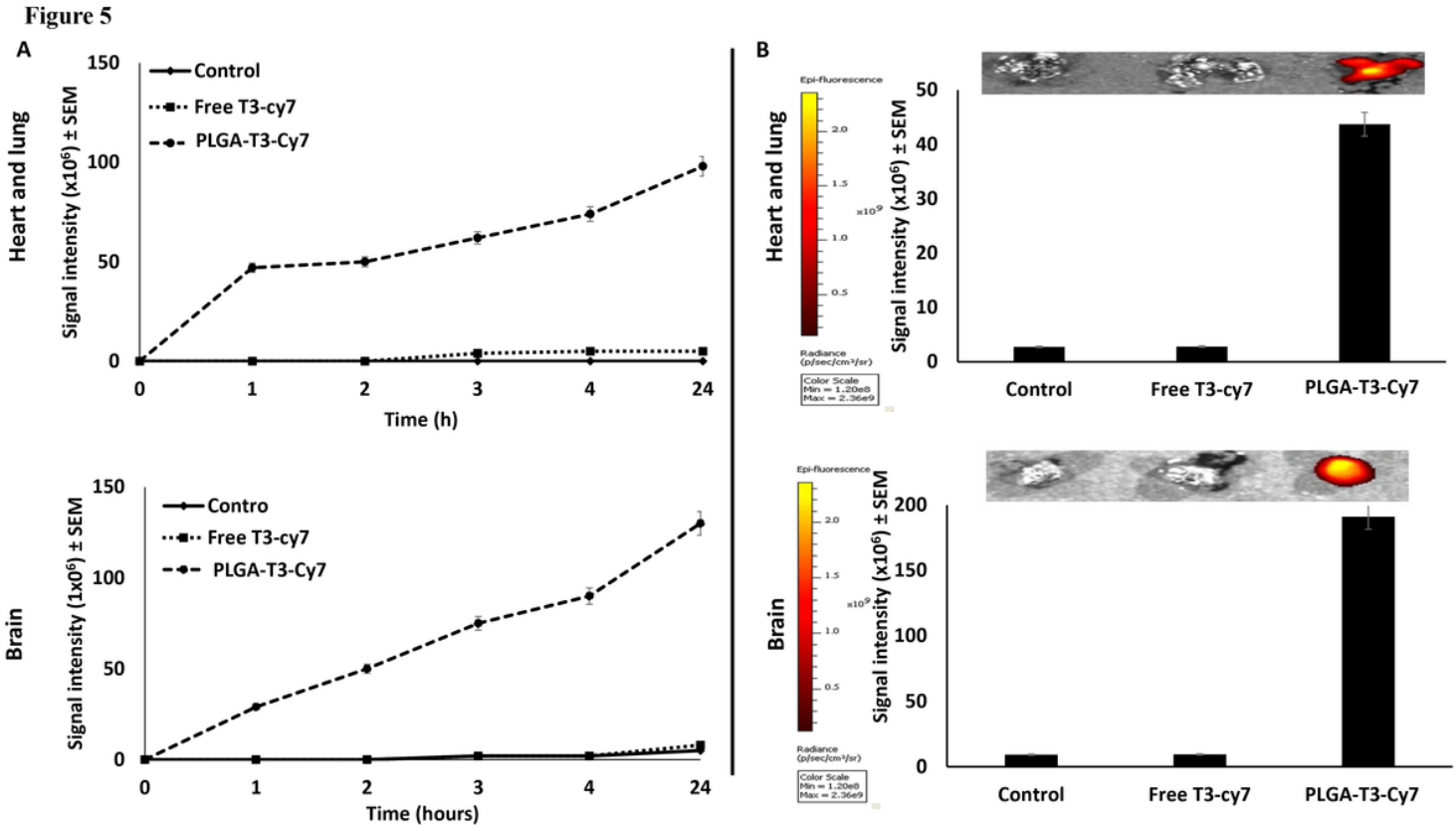

Figure 5

Free T3-Cy7 and PLGA-T3-Cy7biodistribution in brain, heart & lungs in mice (BALB/C) after injection of 300 ul subcutaneously. Cy7 signals detected with IVIS at excitation/emission maximum 750/776 nm wavelength. IVIS images taken to detect Cy7 signals during the following time: A) Before injection, immediately, 1, 2, 3, 4 and 24 h. B) Sacrificed at 24h. Brain, heart & lung Cy7 signals imaged ex vivo.

Supplementary Files

This is a list of supplementary files associated with this preprint. Click to download.

- SupplemenatryMaterials.docx
- Graphicalabstract.pptx
- schema1.png